PNAS RESEARCH ARTICLE | IMMUNOLOGY AND INFLAMMATION

NKp46$^+$ ILC3s promote early neutrophil defense against *Clostridioides difficile* infection through GM-CSF secretion

José L. Fachi[a], Sarah de Oliveira[b], Susan Gilfillan[a], Alina Ulezko Antonova[a], JinChao Hou[c], Marco A. R. Vinolo[b], and Marco Colonna[a,1]

Affiliations are included on p. 9.

Contributed by Marco Colonna; received August 9, 2024; accepted October 2, 2024; reviewed by Marco A. Cassatella and Jay Kolls

Clostridioides difficile **infection (CDI) is a common cause of antibiotic-associated colitis. *C. difficile* proliferates and produces toxins that damage the colonic epithelium, leading to symptoms ranging from mild diarrhea to severe pseudomembranous colitis. The host's innate response to CDI occurs in two phases: an early phase in which neutrophils reduce the bacterial load and a late phase involving repair mechanisms to restore epithelial integrity. Group 3 innate lymphoid cells (ILC3s) are crucial in protecting the gut from CDI. Previous studies have shown that ILC3-derived IL-22 is essential in the late phase of CDI for epithelial repair and maintaining an intestinal microbiota that competes with *C. difficile*, preventing its expansion. Our study finds that ILC3s also protect during the early stages of CDI by sustaining neutrophils through GM-CSF. Less neutrophil production, accumulation, and activation was evident in ILC3-deficient mice than in wild-type (WT) mice, which led to exacerbated symptoms, impaired pathogen clearance, a compromised epithelial barrier, and increased mortality. The adoptive transfer of ILC3s into ILC3-deficient mice restored neutrophil responses and improved disease outcomes. Both in vitro and in vivo experiments revealed that GM-CSF production by ILC3s is crucial for neutrophil production and effective resistance during CDI. Using mice lacking NKp46$^+$ ILC3s, we found that this subset significantly contributes to GM-CSF production in CDI. These findings highlight the critical role of the ILC3-neutrophil connection in early innate responses to CDI. Enhancing ILC3 production of GM-CSF could be a promising strategy for improving host defense against CDI and other enteric infections.**

innate lymphoid cells | GM-CSF | neutrophils | colitis | *Clostridioides difficile*

Significance

Clostridioides difficile infections (CDI) are a major public health issue, particularly in hospitals where antibiotic use is prevalent. Antibiotics disrupt the gut's healthy bacteria, allowing *C. difficile* to flourish and produce harmful toxins, leading to symptoms from mild diarrhea to severe colitis. The recurrent nature of CDI and the emergence of antibiotic-resistant strains complicate treatment. Our research reveals that a type of immune cell, group 3 innate lymphoid cells (ILC3s), not only aids in gut repair during later stages of CDI through the production of IL-22 but also supports early defense by producing GM-CSF, which sustains neutrophil production and activity. Enhancing ILC3 production of GM-CSF could improve treatments for CDI and similar gut infections.

Clostridioides difficile is an anaerobic, Gram-positive bacterium responsible for antibiotic-associated diarrhea and colitis (1, 2). *C. difficile* infections (CDI) present a significant public health challenge, especially in healthcare settings where antibiotic use is common (3, 4). CDI starts when antibiotics disrupt the healthy gut microbiota, reducing its ability to inhibit *C. difficile* growth (5). This disruption allows *C. difficile* to thrive and produce toxins, such as toxin A (enterotoxin) and toxin B (cytotoxin), which are central to the disease's pathology (6, 7). These toxins cause extensive damage to the colonic epithelium, leading to symptoms that range from mild diarrhea to severe pseudomembranous colitis (8). The recurrent nature of CDI and the rise of antibiotic-resistant strains present significant treatment challenges. Despite advances in understanding the microbiological and clinical aspects of CDI, the exact role of the host immune response during the early stages of infection remains incompletely understood.

Host defense against CDI relies heavily on innate immune mechanisms. In mice, the early response on days 1 and 2 postinfection (p.i.) is characterized by rapid neutrophil recruitment to the infection site, which helps control the bacterial load (9, 10). Recruitment and activation of neutrophils are regulated by various cytokines, including granulocyte-macrophage colony-stimulating factor (GM-CSF), a key mediator of neutrophil function (11–15). Later responses, occurring around 4 d p.i., involve resolution and tissue repair (16). These processes depend partly on group 3 innate lymphoid cells (ILC3s) (17, 18). These RORγt-dependent lymphocytes enhance epithelial barrier function and facilitate tissue repair by producing IL-22 in response to tissue alarmins such as IL-23 and IL-1β (19–21).

In mice, ILC3s comprise three distinct subsets (22, 23). The CCR6$^+$ lymphoid tissue inducer (LTi) cells promote lymphoid organogenesis and produce more IL-17 than IL-22. Conversely, NKp46$^+$ ILC3s and their immediate precursors, CCR6$^-$ NKp46$^-$ ILC3s, mainly produce IL-22 rather than IL-17 (24–26). Notably, ILC3s also produce GM-CSF (27). It remains unclear whether this function of ILC3s is relevant to the early immune response against *C. difficile* infection (CDI). In this study, we investigated the role of ILC3s in early host defense against *C. difficile*. We examined the accumulation and

Author contributions: J.L.F., M.A.R.V., and M.C. designed research; J.L.F., S.d.O., and S.G. performed research; J.L.F., A.U.A., and J.H. analyzed data; and J.L.F. and M.C. wrote the paper.

Reviewers: M.A.C., Universita degli Studi di Verona; and J.K., Tulane University.

The authors declare no competing interest.

[1]To whom correspondence may be addressed. Email: mcolonna@wustl.edu.

This article contains supporting information online at https://www.pnas.org/lookup/suppl/doi:10.1073/pnas.2416182121/-/DCSupplemental.

Published October 30, 2024.

activation of ILC3s in the colonic lamina propria following infection and assessed the impact of their deficiency on neutrophil responses, disease severity, and epithelial barrier integrity. Our findings highlight the critical role of ILC3s in sustaining early neutrophil responses to CDI through GM-CSF both locally and in the bone marrow (BM). These results enhance our understanding of the broader functions of innate lymphoid cells in gut immunity and suggest that enhancing ILC3 production of GM-CSF could be a promising strategy for improving host defense against CDI and other enteric infections.

Results

CDI Is Associated With Accumulation of ILC3s that Enhances Resistance to Infection. We investigated how ILC3s impact the early immune response to CDI. After inducing dysbiosis with antibiotics, we infected C57BL/6 mice with 10^8 CFU of *C. difficile* (Fig. 1*A*). The mice were killed 2 d after infection (p.i.) to analyze ILC frequencies in the colonic lamina propria (Fig. 1*B*). We found an increase in the total number of CD45$^+$ leukocytes (Fig. 1*C*), with notable rises in the ILC1 and ILC3 populations (Fig. 1*D*). Specifically, the relative frequency of NKp46$^+$ ILC3s expanded, while CCR6$^+$ ILC3s declined (Fig. 1*E*). We next examined the outcome of CDI in *Rorc*^{Cre} x *Ahr*$^{fl/fl}$ mice (referred to as RORγt$^{\Delta Ahr}$), which have a marked reduction of ILC3s, particularly NKp46$^+$ ILC3s (28, 29) (Fig. 2 *A* and *B*). *Ahr*$^{fl/fl}$ (referred to as wild-type, WT) served as controls. RORγt$^{\Delta Ahr}$ mice had lower survival rates, greater weight loss, and more severe clinical scores compared to WT mice (Fig. 2 *C*–*E*). By day 3 p.i., WT mice began to stabilize in terms of weight and clinical scores, suggesting recovery in the surviving animals. In contrast, RORγt$^{\Delta Ahr}$ mice showed delayed recovery and continued deteriorating. In addition, RORγt$^{\Delta Ahr}$ mice harbored more substantial *C. difficile* burdens on day 4 p.i. (Fig. 2*F*), suggesting poorer pathogen clearance. Increased shortening of the colon but not the cecum was also noted in the RORγt$^{\Delta Ahr}$ mice during infection (Fig. 2 *G*–*I*). Moreover, infected RORγt$^{\Delta Ahr}$ mice had higher FITC-Dextran levels in the blood after oral gavage (Fig. 2*J*) and more extensive bacterial translocation to peripheral organs, including the mesenteric lymph nodes, liver, and spleen (Fig. 2*K*), than did infected WT mice; these observations are consistent with more extensive gut barrier disruption. Tissue damage and loss of goblet cells were also more pronounced on day 4 p.i. in RORγt$^{\Delta Ahr}$ mice (Fig. 2 *L*–*O*), indicating diminished ability to recover from the infection. We conclude that ILC3s are essential for mounting an effective early response by the host against CDI.

Neutrophil Infiltration and Maturation are Impaired in RORγt$^{\Delta Ahr}$ Mice during CDI. Since the early host responses to CDI in mice primarily rely on phagocytes (10, 30, 31), we examined the frequency of these cells in the colonic lamina propria on day 2 p.i. (*SI Appendix*, Fig. S1*A*). We found that neutrophils were the predominant population accumulating during early infection (*SI Appendix*, Fig. S1*B*). Moreover, we noted a positive correlation between neutrophil and ILC3s, specifically NKp46$^+$ ILC3s, in the colonic lamina propria (*SI Appendix*, Fig. S1 *C* and *D*), suggesting potential interactions during CDI. This hypothesis was corroborated by the observation that fewer neutrophils

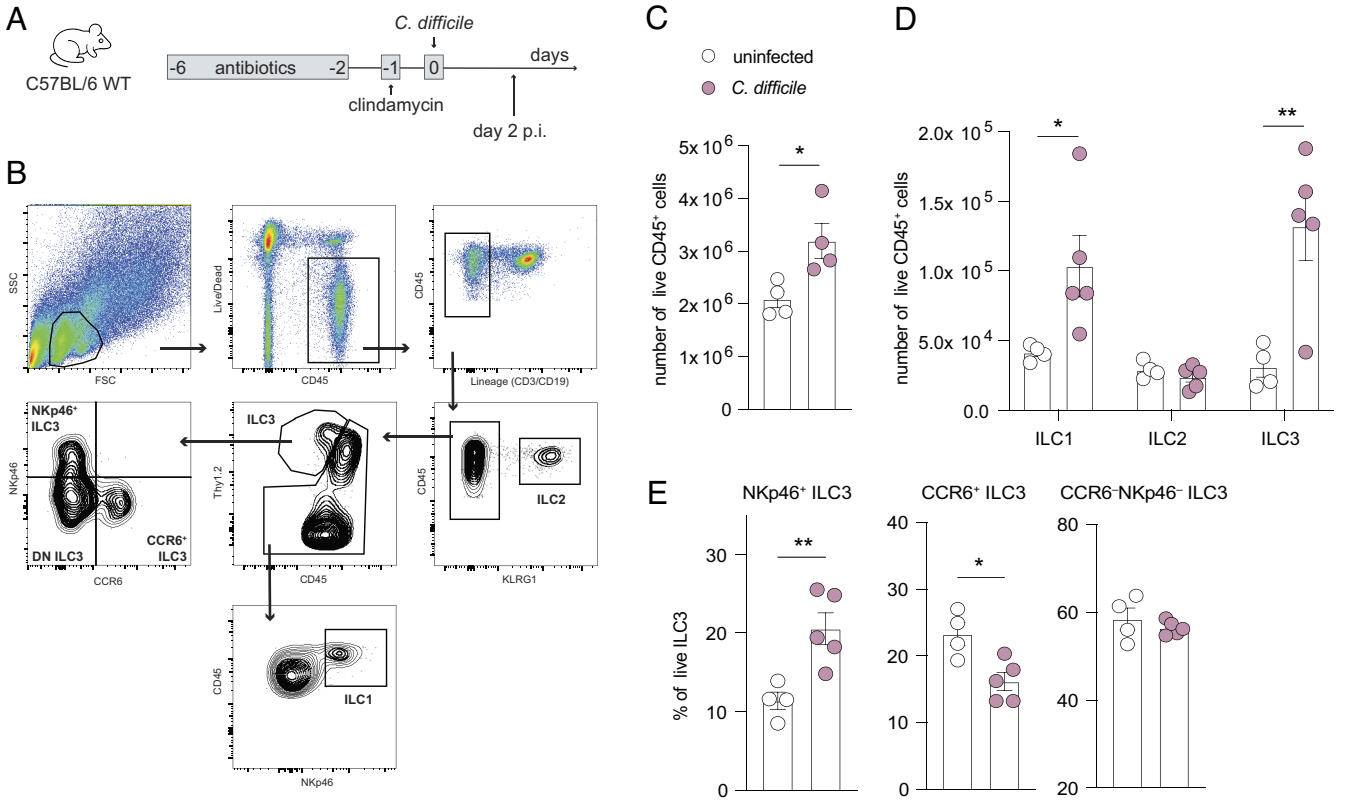

Fig. 1. ILC numbers and frequencies in colonic lamina propria 2 d p.i. (*A*) Schematic representation of CDI. Mice received an oral 4-d antibiotic treatment via drinking water, followed by a single intraperitoneal dose of clindamycin, and subsequently were infected with 10^8 CFU of *C. difficile*. (*B*) FACS strategy for assessing ILC frequency in the colonic lamina propria at day 2 p.i. Lymphocyte-sized cells were gated as live CD45$^+$ and lineage-negative (CD3, CD5, and CD19). ILC2s were identified as KLRG1$^+$, ILC3s as Thy1.2$^+$ CD45 intermediate, and ILC1s as NKp46$^+$ cells excluded from ILC2 and ILC3 gates. Additionally, ILC3 subsets were further characterized as NKp46$^+$, CCR6$^+$, and double-negative. (*C* and *D*) Absolute numbers of total CD45+ cells (*C*) and ILC1s, ILC2s, and ILC3s (*D*) in the colon at day 2 p.i. (n = 4 to 5). (*E*) Frequency of ILC3 subsets in the colonic lamina propria at day 2 p.i. (n = 4 to 5). Data are presented as mean ± SEM. Statistical significance was determined using a two-tailed Student's *t* test (*$P < 0.05$, **$P < 0.01$).

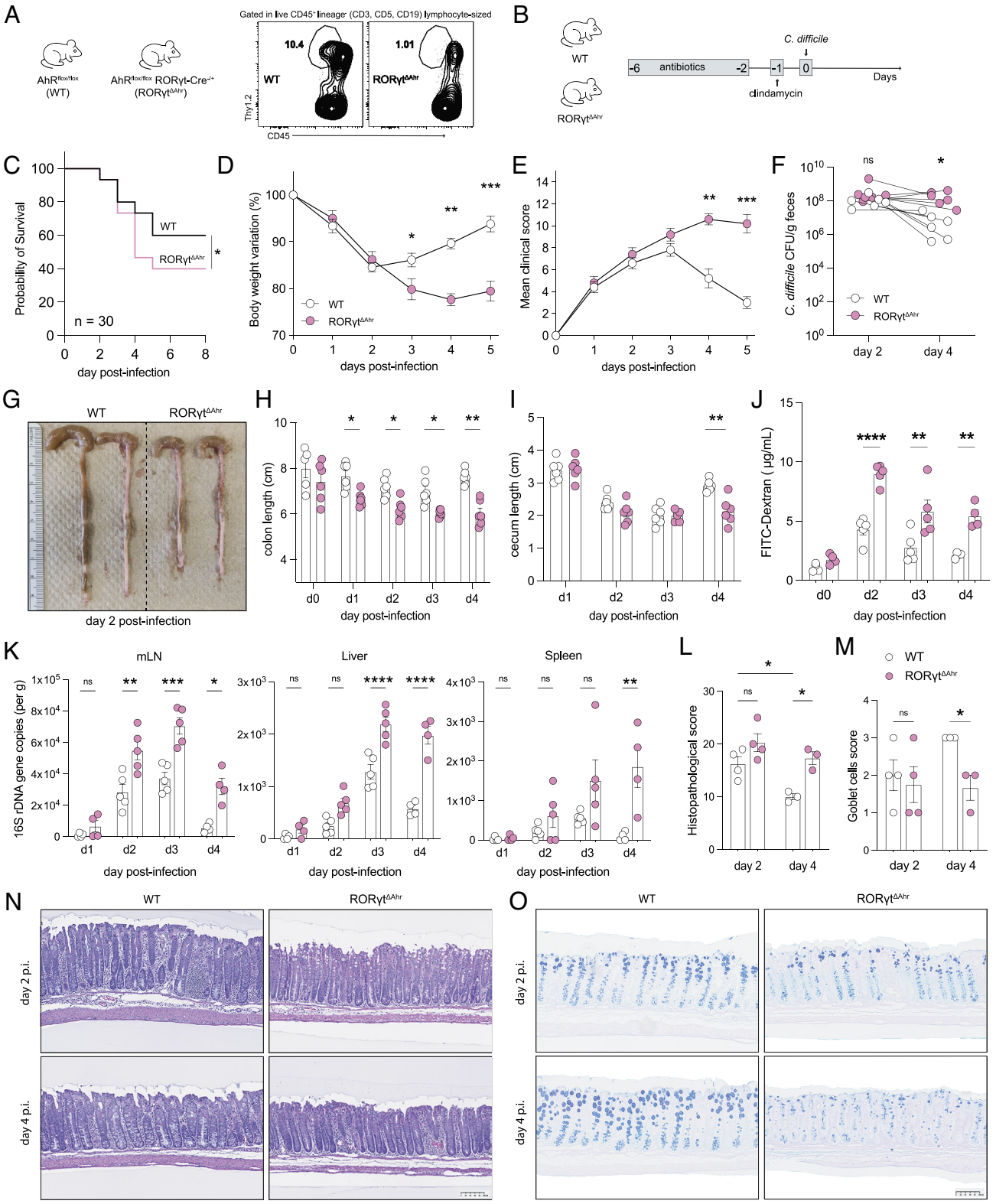

Fig. 2. RORγt$^{\Delta Ahr}$ mice are more susceptible to CDI. (*A*) FACS plot showing the percentage of colonic ILC3s in AhR$^{fl/fl}$ (WT) and AhR$^{fl/fl}$ RORγt-Cre (RORγt$^{\Delta Ahr}$) mice. (*B*) Schematic representation of the CDI protocol: Mice received a mixture of antibiotics in the drinking water for 4 d, followed by a single intraperitoneal dose of clindamycin, and were subsequently infected with 10^8 CFU of *C. difficile*. (*C*–*E*) Outcomes postinfection: probability of survival (*C*), body weight variation (*D*), and mean clinical score (*E*) in WT and RORγt$^{\Delta Ahr}$ mice. Data represent mean ± SEM from three independent experiments (n = 30). (*F*) *C. difficile* burden in fecal pellets of infected mice at days 2 and 4 p.i. (n = 6). (*G*) Representative images of large intestines from mice infected with *C. difficile* at day 2 p.i.(n = 2). (*H* and *I*) Colon (*H*) and cecum (*I*) length on days noted pre- and postinfection (n = 6). (*J*) Gut permeability assessed by FITC-Dextran quantification in blood after 4 h gavage on days noted pre- and postinfection (n = 4 to 5). (*K*) Bacterial translocation quantified by 16S rDNA gene copies in mesenteric lymph nodes (mLN), liver, and spleen normalized by 16S rDNA of *E. coli* on days noted p.i. (n = 4 to 6). (*L*) Histopathological scoring of colonic H&E sections at days 2 and 4 p.i. (n = 3 to 4). The total score ranges from 0 to 30, calculated as the sum of 10 parameters, each quantified on a scale from 0 (normal) to 3 (severe). (*M*) Goblet cell density was scored on a scale from 0 to 3, where 0 indicates absence and 3 indicates profuse enrichment (n = 3 to 4). (*N* and *O*) Representative images of colonic sections stained with H&E (*N*) and Alcian-Blue PAS (*O*) from WT and RORγt$^{\Delta Ahr}$ mice at days 2 and 4 p.i. (Scale bars, 100 µm.) Data represent mean ± SEM. Statistical significance was determined using a two-tailed Student's *t* test (*$P < 0.05$, **$P < 0.01$, ***$P < 0.001$, ****$P < 0.0001$).

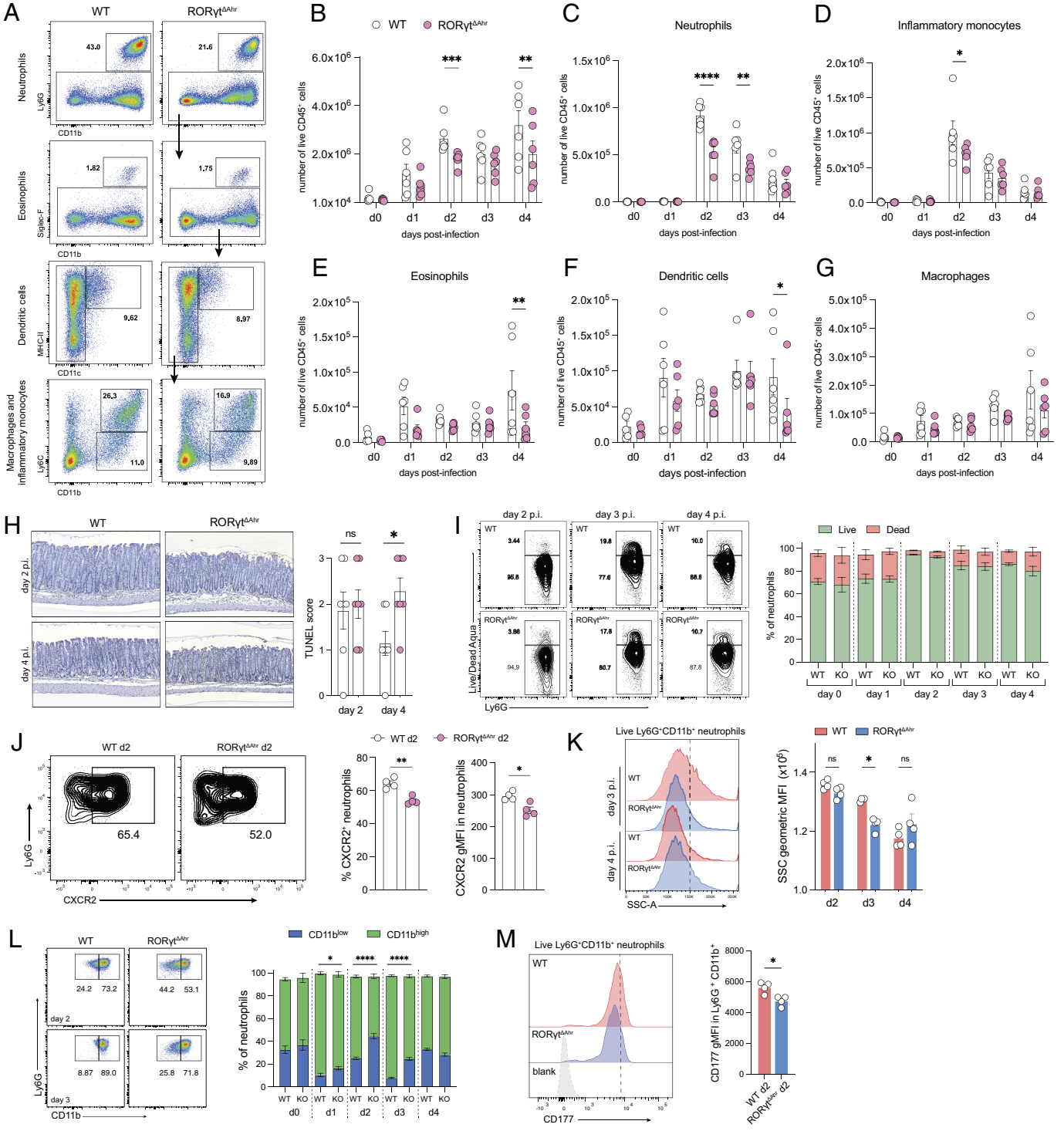

Fig. 3. ILC3 deficiency impairs neutrophil infiltration and function in the colon during CDI. (*A*) Representative FACS plot illustrating the gating strategy used to evaluate myeloid cells from the colonic lamina propria of WT and RORγt$^{\Delta Ahr}$ mice during CDI. (*B–G*) Absolute number of cells in the lamina propria of the colon at different days p.i.: total CD45$^+$ cells (*B*), CD11b$^+$ Ly6G$^+$ neutrophils (*C*), CD11b$^+$ Ly6C$^+$ inflammatory monocytes (*D*), CD11b$^+$ Siglec-F$^+$ eosinophils (*E*), CD11c$^+$ MHC-II$^+$ dendritic cells (*F*), and CD11b$^+$ Ly6C$^-$ macrophages (*G*). Data represent mean ± SEM from two independent experiments (n = 5 to 6). (*H*) Representative sections of the colon stained for TUNEL (*Left*) and quantification by scoring (*Right*) from 0 (normal) to 3 (severe) at days 2 and 4 p.i. (n = 6 to 7). (*I*) Representative FACS plot (*Left*) and quantification (*Right*) of live/dead Ly6G$^+$ CD11b$^+$ neutrophils on days noted p.i. (n = 6). (*J*) FACS plot (*Left*) and quantification (*Right*) of CXCR2 expression on Ly6G$^+$ neutrophils from colonic lamina propria from WT and RORγt$^{\Delta Ahr}$ mice on day 2 p.i. (n = 4). (*K*) Side scatter (SSC) of Ly6G$^+$ CD11b$^+$ neutrophils expressed as geometric mean fluorescence intensity (gMFI), indicating granularity (n = 4). (*L*) FACS plot (*Left*) and quantification (*Right*) of CD11b intensity on Ly6G$^+$ neutrophils, indicating maturation (n = 4). (*M*) CD177 expression intensity on Ly6G$^+$ CD11b$^+$ neutrophils, indicating activation (n = 4). Data represent mean ± SEM. Statistical significance was determined using a two-tailed Student's *t* test (*P < 0.05, **P < 0.01, ***P < 0.001, ****P < 0.0001).

accumulated in RORγt$^{\Delta Ahr}$ mice than in WT mice during the early phase, although other myeloid cells were also impacted (Fig. 3 *A–G*). T cells are crucial in directing neutrophil migration during bacterial lung infections, mainly by producing IL-17 and IL-22 (32, 33). However, in the colonic lamina propria of *Rag1*$^{-/-}$ (*SI Appendix*, Fig. S2 *A–C*) and *Tcrb*$^{-/-}$ mice (*SI Appendix*, Fig. S2 *D–F*), which lack adaptive immune responses, neutrophil accumulation was comparable to that of WT mice. These results

suggest a specific association between ILC3 deficiency and impaired neutrophil accumulation in early CDI.

To determine whether the reduced early neutrophil accumulation in RORγt$^{\Delta Ahr}$ mice during CDI was due to cell death, we performed TUNEL staining on colon sections (Fig. 3*H*). On day 2 p.i., when neutrophil infiltration occurs, ILC3-deficient mice showed similar levels of cell death as WT mice. Only by day 4, we observed a slight increase in cell death in the lamina propria of RORγt$^{\Delta Ahr}$ mice. Flow cytometric analysis of neutrophils from the colon of WT and RORγt$^{\Delta Ahr}$ corroborated no significant differences in neutrophil viability between the two genotypes during CDI (Fig. 3*I*), suggesting that the early reduction of neutrophil numbers is not due to increased cell death. However, neutrophils in the colonic lamina propria of RORγt$^{\Delta Ahr}$ mice had lower CXCR2 expression (Fig. 3*J*), a crucial receptor for neutrophil release from the BM and tissue infiltration (34). CXCR2 levels reflect neutrophil maturation and migration capacity. Additionally, these neutrophils showed decreased granularity at day 3 p.i. compared to WT mice, as indicated by lower side scatter (SSC) intensity (Fig. 3*K*), corroborating reduced maturation. Lower expression of CD11b (Fig. 3*L*) and CD177 (Fig. 3*M*), markers of neutrophil maturation and activation, further supported this. On day 2 p.i., RORγt$^{\Delta Ahr}$ mice had more CD11b^{low} and fewer CD11b^{high} neutrophils with low CD177 levels compared to WT mice. These findings suggested that the reduced neutrophil presence in the colonic lamina propria of RORγt$^{\Delta Ahr}$ mice may be due to impaired neutrophil production and maturation.

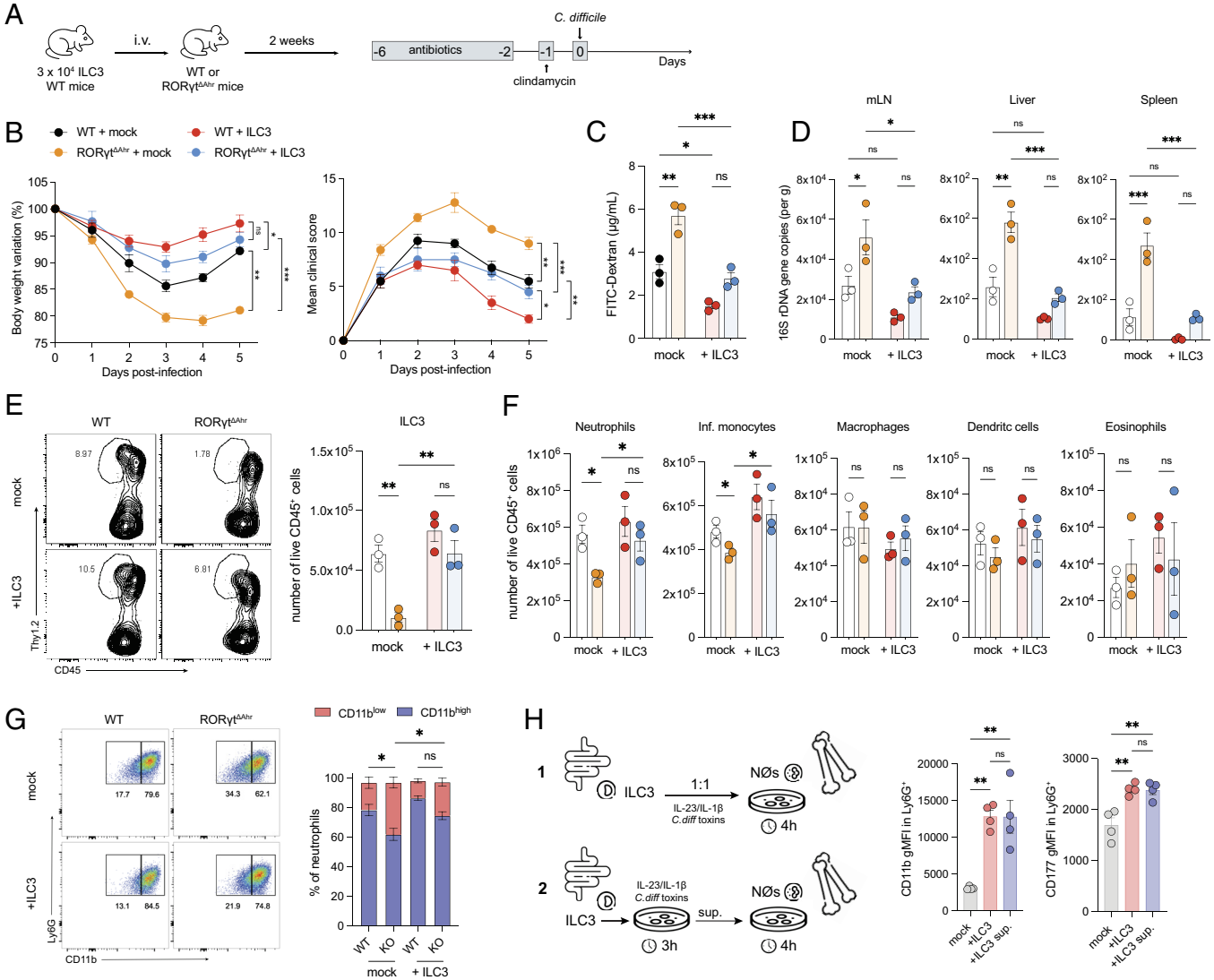

Fig. 4. Adoptive transfer of ILC3s rescues neutrophil function during CDI. (*A*) Schematic representation of adoptive transfer of ILC3s into RORγt$^{\Delta Ahr}$ and WT mice prior to CDI: ILC3s were FACS-sorted from the small intestine and colon of WT mice at steady-state, and 3 × 10^4 cells intravenously transferred into both WT and RORγt$^{\Delta Ahr}$ mice. Following a 2-wk reconstitution period, mice underwent antibiotic treatment and CDI. Experimental groups included WT + mock (WT mice receiving PBS), RORγt$^{\Delta Ahr}$ + mock (RORγt$^{\Delta Ahr}$ mice receiving PBS), WT + ILC3 (WT mice receiving ILC3s), and RORγt$^{\Delta Ahr}$ + ILC3 (RORγt$^{\Delta Ahr}$ mice receiving ILC3s). (*B*) Body weight variation (*Left*) and mean clinical score (*Right*) during CDI (n = 5). (*C*) Gut permeability assessed by serum quantification of FITC-Dextran at day 2 p.i. (n = 3). (*D*) Bacterial translocation detected by 16S rDNA gene copies in mesenteric lymph nodes (mLN), liver, and spleen at day 2 p.i. (n = 3). (*E*) FACS plot (*Left*) and absolute number (*Right*) of ILC3s in the colon at day 2 p.i. (n = 3). (*F*) Absolute number of neutrophils, inflammatory monocytes (Ly6C$^+$), macrophages, dendritic cells, and eosinophils in the lamina propria of the colon on day 2 p.i. (n = 3). (*G*) FACS plot (*Left*) and quantification (*Right*) of neutrophil maturation by CD11b expression intensity following adoptive transfer of ILC3s (n = 3). (*H*) Schematic of ILC3 and neutrophil coculture: ILC3s were FACS-sorted from the small intestine and cocultured for 4 h with Percoll-purified BM neutrophils in the presence of IL-23, IL-1β, and *C. difficile* toxins (1). Alternatively, sorted ILC3s were cultured for 3 h with IL-23, IL-1β, and *C. difficile* toxins, and the supernatant was used to stimulate Percoll-purified BM neutrophils for 4 h (2). Neutrophil maturation and activation were evaluated by CD11b and CD177 expression intensity, respectively (n = 4). Data represent mean ± SEM. Statistical significance was determined using a two-tailed Student's *t* test (*B*–*G*) and one-way ANOVA with post hoc Tukey test (*H*) (*$P < 0.05$, **$P < 0.01$, ***$P < 0.001$).

ILC3 Deficiency Affects BM Granulopoiesis during CDI. To confirm the role of ILC3s in regulating neutrophil production and maturation, we examined BM neutrophils in WT and RORγt$^{\Delta Ahr}$ mice on day 0 and day 2 p.i. (*SI Appendix*, Fig. S3*A*). There were no significant differences in total neutrophil counts between WT and RORγt$^{\Delta Ahr}$ mice on day 0 (*SI Appendix*, Fig. S3*B*). Infected WT mice had significantly higher neutrophil counts compared to uninfected WT controls. In contrast, neutrophil counts did not increase in infected RORγt$^{\Delta Ahr}$ mice (*SI Appendix*, Fig. S3*B*). We analyzed neutrophil maturation stages and found that CDI induced granulopoiesis in WT mice, demonstrated by increased percentages of pre-neutrophils and mature neutrophils, along with a trend toward higher levels of immature neutrophils (*SI Appendix*, Fig. S3 *C–E*). Conversely, the percentage of aged neutrophils was reduced in these infected WT mice (*SI Appendix*, Fig. S3*F*). In RORγt$^{\Delta Ahr}$ mice, there was no increase in immature and pre-neutrophils. Moreover, although the frequency of mature neutrophils was similar to that in infected WT mice, the proportion of aged neutrophils was higher, suggesting impaired bone marrow neutrophil production and release (*SI Appendix*, Fig. S3 *C–F*). RORγt$^{\Delta Ahr}$ mice also exhibited a reduced number of BM neutrophils expressing CXCR2 (*SI Appendix*, Fig. S3*G*), consistent with the observation in the colon (Fig. 3*J*), highlighting the impaired neutrophil maturation.

To further investigate granulopoiesis, we examined hematopoietic progenitors in the BM (*SI Appendix*, Fig. S4*A*). Hematopoietic stem cells (HSCs) and multipotent progenitor 1 (MPP1) populations were similar in uninfected and infected WT and RORγt$^{\Delta Ahr}$ mice. However, MPP2 frequencies decreased in both infected groups (*SI Appendix*, Fig. S4*C*). Notably, WT mice had a significant increase in MPP3 on day 2 p.i., whereas RORγt$^{\Delta Ahr}$ mice did not (*SI Appendix*, Fig. S4*C*); a similar pattern was seen for granulocyte-monocyte progenitors (GMPs) (*SI Appendix*, Fig. S4*D*). Finally, no differences were noted in the frequencies of common myeloid progenitors (CMPs) (*SI Appendix*, Fig. S4*E*). Overall, our data indicate that ILC3 deficiency selectively impairs the production, maturation, and release of neutrophils from the BM during early CDI.

ILC3 Adoptive Transfer Restores Neutrophil Levels in RORγt$^{\Delta Ahr}$ Mice During CDI. To investigate whether ILC3s are crucial for early resistance to CDI, we adoptively transferred sorted intestinal ILC3s into either WT or RORγt$^{\Delta Ahr}$ mice. After a two-week reconstitution period, the mice were treated with antibiotics and infected with *C. difficile* (Fig. 4*A*). WT mice that received ILC3s were more protected than those given a placebo (Fig. 4*B*). In RORγt$^{\Delta Ahr}$ mice, transfer of ILC3s resulted in less body weight loss and improved clinical scores compared to those receiving a placebo (Fig. 4*B*). ILC3 transfer improved epithelial barrier integrity on day 2 p.i., as shown by decreased permeability to FITC-Dextran (Fig. 4*C*) and reduced bacterial translocation to mesenteric lymph nodes, liver, and spleen (Fig. 4*D*). Reconstituted ILC3s were confirmed in the colonic lamina propria of these mice on day 2 p.i. (Fig. 4*E*). Additionally, ILC3 reconstitution in RORγt$^{\Delta Ahr}$ mice restored neutrophil accumulation to numbers similar to those in WT mice, without affecting other myeloid cell types (Fig. 4*F*). ILC3-reconstitution enhanced maturation of neutrophils in comparison to those receiving a placebo (Fig. 4*G*).

To further investigate the interaction between ILC3s and neutrophils, we conducted two parallel experiments using sorted intestinal ILC3s: (1) direct coculture with BM-derived neutrophils and (2) addition of ILC3-conditioned medium to neutrophils in vitro. In both cases, ILC3s were stimulated with IL-23, IL-1β, and *C. difficile* toxins prior to or during the experiment (Fig. 4*H*). Both methods resulted in enhanced neutrophil maturation and activation, as indicated by increased CD11b and CD177 expression (Fig. 4*H*). These findings suggest that ILC3s secrete soluble factors that promote neutrophil function. To investigate these factors, we performed bulk RNA sequencing (RNAseq) on ILC3s isolated from the colon lamina propria of WT mice on days 0 and 2 p.i. through cell sorting (*SI Appendix*, Fig. S5*A*). The analysis showed that CDI led to increased mRNA expression of several cytokines in ILC3s, including *Il22*, *Il17a*, *Tnf*, *Csf2* (encoding GM-CSF), *Cxcl2*, *Cxcl5*, *Ccl2*, and *Ccl20* (*SI Appendix*, Fig. S5*B*). Among these, CXCL2 is a known chemoattractant for neutrophils, while CSF2 serves as a trophic factor for them. We confirmed the upregulation of IL-22, IL-17, IFNγ, TNFα, CCL2, and CXCL2 in ILC3s from infected WT mice on day 2 p.i. using flow cytometry (*SI Appendix*, Fig. S5*C*). To determine whether ILC3s are a key source of these cytokines and chemokines in the colon during CDI, we analyzed their intracellular content in total CD45$^+$ cells from the colon. CDI significantly increased the percentage of CD45$^+$ cells producing IL-22, IL-17, IFNγ, TNFα, CXCL2, and CCL2. In contrast, RORγt$^{\Delta Ahr}$-infected mice had significantly fewer cytokine-expressing cells in the colonic lamina propria on day 2 p.i. (*SI Appendix*, Fig. S5*D*), highlighting ILC3s as a key source of cytokines and chemokines during CDI, some of which may act as chemoattractant (CXCL2) or growth factor (GM-CSF) for neutrophils.

ILC3-Derived GM-CSF Promotes Neutrophil Responses During CDI. Among the cytokines produced by ILC3s in response to *C. difficile*, we focused on GM-CSF for its critical role in promoting the production and maturation of neutrophils from hematopoietic progenitors (35), as well as supporting neutrophil survival and activation in both mice (15, 36) and humans (37). Additionally, ILC3-derived GM-CSF has been shown to induce intestinal macrophage responses (27, 38). We confirmed a significant increase in GM-CSF-producing ILC3s in WT mice on day 2 of CDI (Fig. 5*A*). This increase was associated with elevated *Csf2* mRNA levels in the proximal colon on days 2 and 3 p.i. (Fig. 5*B*). In contrast, RORγt$^{\Delta Ahr}$ mice had lower *Csf2* mRNA levels during infection (Fig. 5*B*), implicating ILC3s as a main source of GM-CSF. Corroborating the importance of GM-CSF for neutrophil responses, GM-CSF-deficient mice (*Csf2*$^{-/-}$) exhibited increased susceptibility to CDI compared to WT mice. This was evidenced by increased body weight loss, worsened clinical scores, increased *C. difficile* burden, bacterial translocation, colon shortening, and exacerbated histopathological scores (*SI Appendix*, Fig. S6 *A–E*).

To confirm that ILC3-derived GM-CSF drives neutrophil responses, we stimulated sorted intestinal ILC3s in vitro with IL-23, IL-1β, and *C. difficile* toxins. We then treated BM-derived neutrophils with the ILC3 culture supernatant, with or without anti-GM-CSF neutralizing antibody and measured neutrophil activation and maturation (Fig. 5*C*). ILC3 culture supernatant induced expression of CD177 and CD11b, which was mitigated by neutralization of GM-CSF (Fig. 5*D*). In vitro coculture of either WT or *Csf2*$^{-/-}$ ILC3s with BM neutrophils confirmed that GM-CSF production by ILC3s is crucial for neutrophil maturation and activation, as assessed by expression of CD11b and CD177, respectively (Fig. 5 *E* and *F*). Finally, adoptive transfer of sorted intestinal WT or *Csf2*$^{-/-}$ ILC3s into WT or RORγt$^{\Delta Ahr}$ mice demonstrated that WT ILC3s improved clinical outcomes and neutrophil accumulation during CDI in RORγt$^{\Delta Ahr}$ mice, whereas *Csf2*$^{-/-}$ ILC3s did not (Fig. 5 *G–K* and *SI Appendix*, Fig. S7 *A–D*). Treatment of infected mice with recombinant GM-CSF mitigated disease outcomes, while neutralizing GM-CSF exacerbated disease severity (Fig. 5*L*), further validating the role of GM-CSF in resistance to CDI. We conclude that GM-CSF is relevant for regulation of immune response during CDI and that ILC3-derived GM-CSF promotes neutrophil responses.

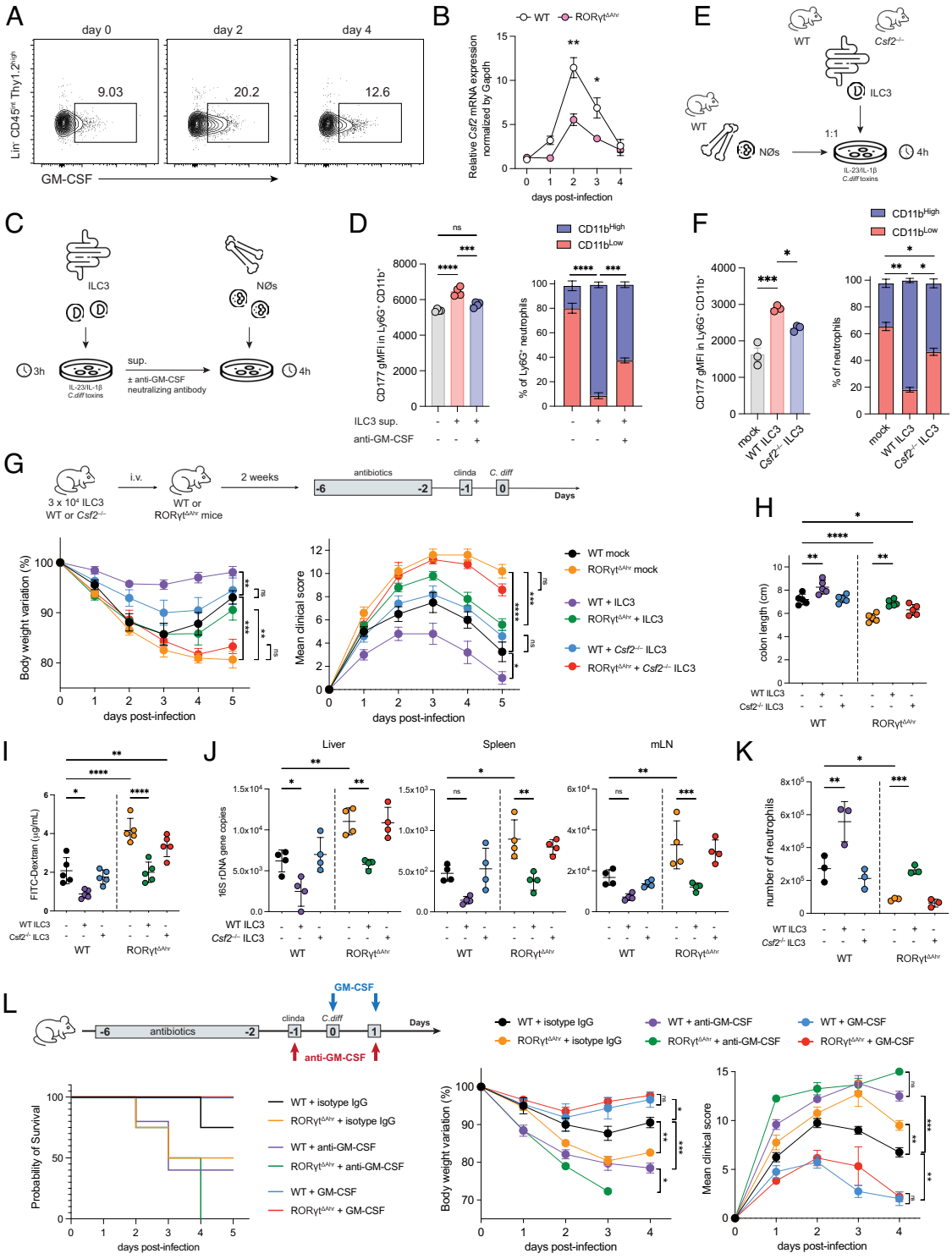

Fig. 5. ILC3-derived GM-CSF is crucial for neutrophil infiltration and function during CDI. (*A*) FACS plot of GM-CSF-producing ILC3s from colonic lamina propria prior to and at 2 and 4 d p.i. (*B*) Relative GM-CSF mRNA (*Csf2*) expression in the proximal colon during CDI in WT and RORγt$^{\Delta Ahr}$ mice (n = 5). (*C*) Schematic representation of BM neutrophil culture in vitro for 4 h with supernatant from stimulated ILC3s, with or without the addition of an anti-GM-CSF neutralizing antibody. ILC3s were FACS-sorted from the small intestine and cultured for 3 h with IL-23, IL-1β, and *C. difficile* toxins. (*D*) Activation and maturation of Ly6G$^+$ neutrophils evaluated by CD177 and CD11b expression, respectively (n = 4). (*E*) Schematic representation of small intestine ILC3s from WT or GM-CSF KO (*Csf2*$^{-/-}$) mice cocultivated with Percoll-purified BM neutrophils at 1:1 ratio for 4 h with IL-23, IL-1β, and *C. difficile* toxins. (*F*) CD177 and CD11b expression intensity in Ly6G$^+$ neutrophils after coculture with WT or *Csf2*$^{-/-}$ ILC3 (n = 3). (*G*) Schematic representation of the adoptive transfer of ILC3s into RORγt$^{\Delta Ahr}$ and WT mice. ILC3s were FACS-sorted from the small intestine of WT or *Csf2*$^{-/-}$ mice at steady-state, and 3 × 10^4 cells were intravenously transferred into both WT and RORγt$^{\Delta Ahr}$ mice. Following a 2-wk reconstitution period, mice received antibiotic and were infected with *C. difficile*. Experimental groups included WT mock (WT mice receiving PBS), RORγt$^{\Delta Ahr}$ mock (RORγt$^{\Delta Ahr}$ mice receiving PBS), WT + ILC3 (WT mice receiving WT ILC3s), RORγt$^{\Delta Ahr}$ + ILC3 (RORγt$^{\Delta Ahr}$ mice receiving WT ILC3s), WT + *Csf2*$^{-/-}$ ILC3 (WT mice receiving *Csf2*$^{-/-}$ ILC3s), and RORγt$^{\Delta Ahr}$ + *Csf2*$^{-/-}$ ILC3 (RORγt$^{\Delta Ahr}$ mice receiving *Csf2*$^{-/-}$ ILC3s). Body weight loss (*Left*) and mean clinical score (*Right*) during CDI (n = 5). (*H*) Colon length on day 2 p.i. (n = 5). (*I*) Gut permeability measured by FITC-Dextran assay on day 2 p.i. (n = 5). (*J*) Bacterial translocation assessed by 16S rDNA gene quantification in the liver, spleen, and mLN (n = 4). (*K*) Absolute number of neutrophils in the lamina propria of the colon 2 d p.i. (n = 3). (*L*) Scheme of treatment with either a neutralizing antibody against GM-CSF or recombinant mouse GM-CSF during CDI; WT and RORγt$^{\Delta Ahr}$ mice were treated. Outcomes postinfection include probability of survival, body weight loss, and mean clinical score (n = 4). Data represent mean ± SEM. Statistical significance was determined using a two-tailed Student's *t* test (*B*) and One-way ANOVA with post hoc Tukey test (*C*–*L*) (*P < 0.05, **P < 0.01, ***P < 0.001, ****P < 0.0001).

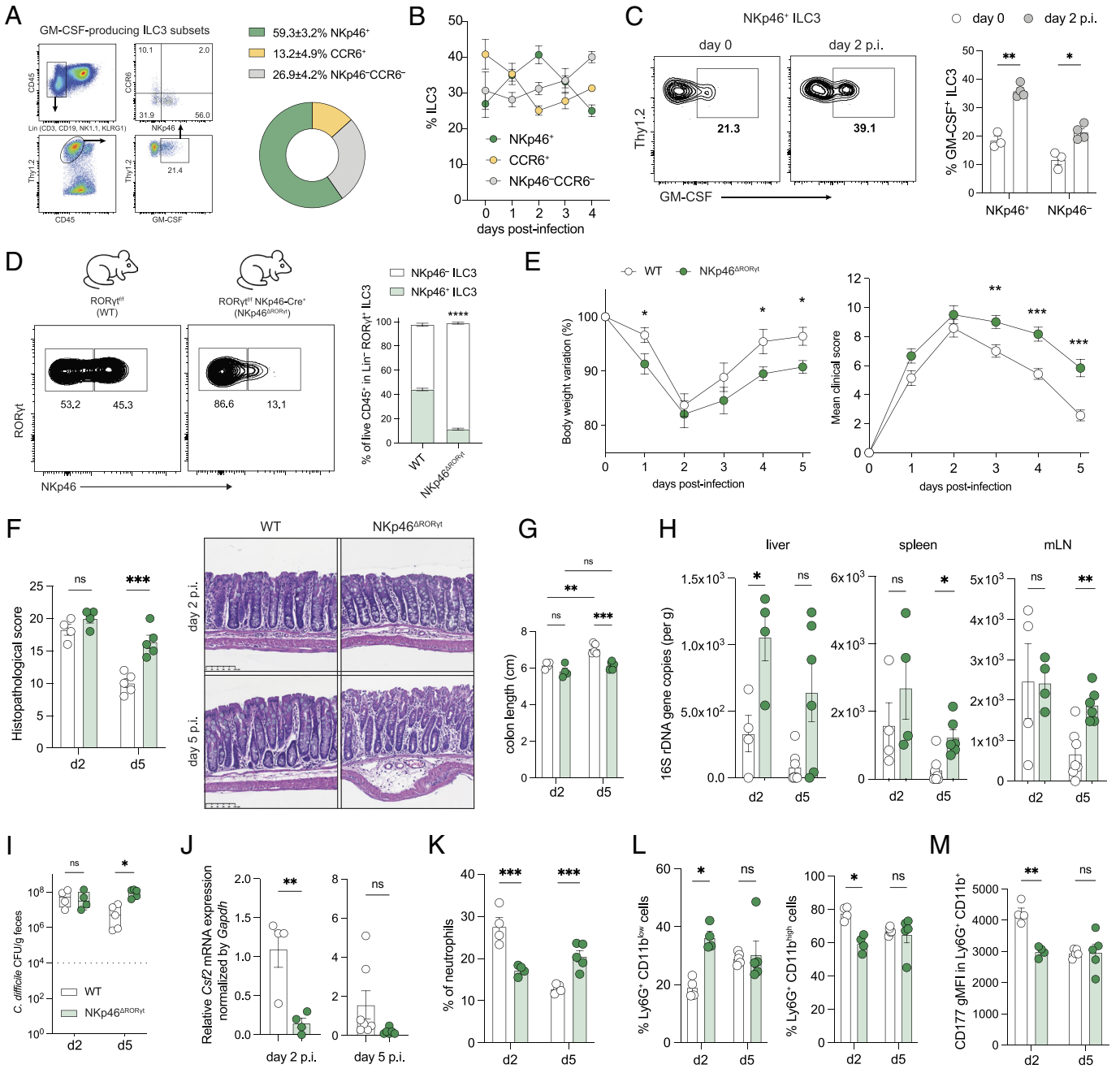

Fig. 6. NKp46$^+$ ILC3s regulate neutrophil responses and enhance mouse resistance to CDI. (*A*) Representative FACS strategy (*Left*) and percentage (*Right*) of GM-CSF production by distinct subsets of ILC3s (n = 4). (*B*) Frequency of NKp46$^+$, CCR6$^+$, and double-negative (NKp46$^-$CCR6$^-$) ILC3s during CDI (n = 4). (*C*) Percentage (*Right*) of GM-CSF production by NKp46$^+$ and NKp46$^-$ ILC3s at day 0 and 2 p.i. (n = 4). A representative FACS plot (*Left*) for NKp46$^+$ ILC3s only is shown. (*D*) Frequency of NKp46$^+$ ILC3s in WT and NKp46$^{\Delta ROR\gamma t}$ mice (ROR$\gamma t^{fl/fl}$ *Ncr1*^{Cre}) (n = 3). (*E*) Body weight variation (*Left*) and mean clinical score (*Right*) during CDI. Data represent mean ± SEM from two independent experiments (n = 8 to 9). (*F*) Histopathological scoring (*Left*) and representative H&E sections of colon (*Right*) at days 2 and 5 p.i. (n = 3 to 4). Score ranges 0 to 30, summing 10 parameters graded in 0 (normal) to 3 (severe). (Scale bars, 100 μm.) (*G*) Colon length at days 2 and 5 p.i. (n = 4 to 5). (*H*) Bacterial translocation quantified by 16S rDNA gene copies in liver, spleen, and mesenteric lymph nodes (mLN) (n = 4 to 6). (*I*) *C. difficile* burden in fecal pellets at days 2 and 5 p.i. (n = 4 to 5). (*J*) Relative expression of *Csf2* mRNA in the proximal colon of WT and NKp46$^{\Delta ROR\gamma t}$ mice at days 2 and 5 p.i. (n = 4 to 6). (*K*) Frequency of Ly6G$^+$ CD11b$^+$ neutrophils in the colonic lamina propria at days 2 and 5 p.i. (n = 4 to 5). (*L*) CD11b expression levels in colonic Ly6G$^+$ neutrophils at days 2 and 5 p.i. (n = 4 to 5). (*M*) CD177 expression intensity in colonic Ly6G$^+$ CD11b$^+$ neutrophils expressed as geometric mean fluorescence intensity (gMFI) (n = 4 to 5). Data represent mean ± SEM. Statistical significance was determined using a two-tailed Student's *t* test (*P < 0.05, **P < 0.01, ***P < 0.001).

NKp46$^+$ ILC3s are the Crucial Subset for GM-CSF-Mediated Protection during CDI. We investigated which ILC3 subsets are responsible for the production of GM-CSF during CDI by performing flow cytometry on lamina propria lymphocytes. We found that NKp46$^+$ ILC3s are the main source of GM-CSF among ILC3 subsets in WT mice on day 2 p.i. (Fig. 6*A*). NKp46$^+$ ILC3s accumulated in the colonic lamina propria during early CDI, whereas CCR6$^+$ and double-negative (CCR6$^-$NKp46$^-$) subsets appeared later (Fig. 6*B*). GM-CSF production was significantly higher in NKp46$^+$ ILC3s than in NKp46$^-$ ILC3s on day 2 p.i. (Fig. 6*C*). GM-CSF production in CD4$^+$ T cells is regulated by STAT3 (39) and STAT5 (40). To explore whether similar mechanisms apply to ILC3s, we examined colonic ILC3s from both uninfected and 2-day p.i. mice. We observed a clear increase in STAT3 phosphorylation (*SI Appendix*, Fig. S8*A*) and a slight increase in STAT5 phosphorylation (*SI Appendix*, Fig. S8*B*),

specifically in NKp46^{+} ILC3s, but not in NKp46^{-} ILC3s. These results suggest that GM-CSF production in ILC3s is induced by mechanisms similar to those in T cells.

To examine the impact of NKp46^{+} ILC3s on the neutrophil response during CDI, we utilized *Ncr1*^{Cre} x *Rorc*$^{fl/fl}$ mice (referred to as NKp46$^{\Delta ROR\gamma t}$ mice), which selectively lack NKp46^{+} ILC3s (41). We confirmed that these mice exhibit reduced frequency of NKp46^{+} ILC3s in the colonic lamina propria (Fig. 6*D*) while maintaining frequencies and numbers of ILC1s, ILC2s, and total ILC3s equivalent to those in WT mice (*SI Appendix*, Fig. S9*A*). These mice exhibited heightened susceptibility to CDI, as demonstrated by accentuated body weight loss coupled with higher clinical scores (Fig. 6*E*), histopathological damage (Fig. 6*F*), colon shortening (Fig. 6*G*), and exacerbated bacterial translocation (Fig. 6*H*). On day 5 p.i., they also carried a higher *C. difficile* burden (Fig. 6*I*), indicating impaired pathogen clearance. Furthermore, there was a significant decrease in *Csf2* mRNA levels in the proximal colon on day 2 p.i. (Fig. 6*J*). Neutrophil accumulation was also reduced in NKp46$^{\Delta ROR\gamma t}$ mice on day 2 p.i. (Fig. 6*K*), whereas other myeloid cell populations remained unaffected (*SI Appendix*, Fig. S9*B*). However, neutrophil accumulation in NKp46$^{\Delta ROR\gamma t}$ mice increased during the later stages of CDI (Fig. 6*K*), a period typically associated with reduced inflammation and tissue recovery (16). Additionally, these mice displayed impaired early neutrophil maturation (Fig. 6*L*) and activation (Fig. 6*M*), as evidenced by lower CD11b and CD177 expression, respectively. Overall, these results indicate that the absence of NKp46^{+} ILC3s leads to increased susceptibility to CDI. This enhanced susceptibility is characterized by reduced GM-CSF production and compromised neutrophil-mediated responses (*SI Appendix*, Fig. S10).

Discussion

ILC3s are established as crucial players in the response against CDI (17, 18, 42). Most studies have shown that ILC3s protect against CDI through IL-22, which facilitates epithelial repair in the late stage and sustains an intestinal microbiota that competes with *C. difficile*, preventing its expansion. Our study reveals the pivotal role of ILC3s in the early innate response to CDI by supporting the generation, maturation, and migration of neutrophils through the release of GM-CSF. ILC3s were abundant in the colonic lamina propria during early CDI, particularly the NKp46^{+} ILC3 subset. This enrichment of colonic ILC3s correlated with the abundance and activation of neutrophils, which are critical for protection against CDI (9, 10, 43). Analysis of RORγt$^{\Delta Ahr}$ and NKp46$^{\Delta ROR\gamma t}$ mice alongside WT controls corroborated that deficiency of ILC3s leads to a weakened neutrophil response during CDI, which was associated with greater disease severity and impaired pathogen clearance. While T and B cells do not seem essential for the early neutrophil response to CDI, their potential roles in host response to CDI during recovery and recurrence still need further investigation.

In a previous study, we found that neutrophils produce IL-1β during CDI, which enhances IL-22 production by ILC3s (17). Together with current data, this highlights the cross talk between ILC3s and neutrophils during CDI. ILC3s secrete GM-CSF, which acts remotely on the BM to promote granulopoiesis, increasing the availability of mature neutrophils that migrate to the infection site. Locally, ILC3-produced GM-CSF supports neutrophil activation. These findings on the beneficial role of GM-CSF production by NKp46+ ILC3s in CDI build on previous research regarding the effects of GM-CSF produced by ILC3s. Previous studies have shown that GM-CSF from NKp46^{+} ILC3s contributes to the accumulation of inflammatory cells and colitis in various models of inflammatory bowel disease (11–13, 41). Moreover, engagement of death receptor 3 (DR3) by TNF-like ligand 1A (TL1A) was shown to promote ILC3 production of GM-CSF, leading to myeloid cell accumulation and exacerbated colitis. Conversely, blocking GM-CSF or IL-23 alleviated colitis, as did neutralizing TL1A (44). GM-CSF secreted by ILC3s was also shown to promote the differentiation of DCs and mononuclear phagocytes that maintain colonic Treg homeostasis (27). In humans, GM-CSF and CXCL8 produced by NCR1^{+} ILC3s influence neutrophil migration and survival, which is vital for the maintenance of early pregnancy (45). Cumulatively, these findings show that the production of GM-CSF by ILC3s may have beneficial or detrimental outcomes depending on the context.

During the early stages of CDI, ILC3s notably produce the chemokine CXCL2, which recruits neutrophils by binding to CXCR2, a receptor specifically expressed on these cells. Thus, GM-CSF and CXCL2 work together to enhance neutrophil recruitment to the site of infection. Additionally, the number of NKp46^{+} ILC3s increased during CDI. Normally, these cells develop from CCR6^{-}NKp46^{-} progenitors through coordinated shifts in the expression of RORγt and T-bet, with RORγt declining and T-bet increasing (24). CDI seems to accelerate this conversion, allowing the innate immune system to rapidly boost GM-CSF, CXCL2, and IL-22 production to fight the infection. While NKp46^{+} ILC3s can fully differentiate into IFN-γ-producing ILC1s through a further increase in the T-bet-to-RORγt ratio (26, 46, 47), it is unclear whether this transition occurs during CDI, as it may require different inflammatory signals in intensity or quality.

In conclusion, our study highlights the crucial role of ILC3s in early immune responses to CDI and underscores the importance of GM-CSF produced by NKp46^{+} ILC3s in activating neutrophils and clearing pathogens. These findings enhance our understanding of gut immune responses to enteric infections and suggest that boosting GM-CSF production by ILC3s could be a promising strategy for improving host defense against CDI and other enteric infections.

Materials and Methods

The detailed experimental procedures, including mouse lineage, the *C. difficile* infection model, isolation of colonic lamina propria cells, isolation of BM cells, quantification of *C. difficile* burden, assessment of intestinal epithelial permeability, bacterial 16S rDNA quantification, histopathological and clinical scoring, adoptive transfer of intestinal ILC3s, bulk RNAseq, in vitro assays, in vivo GM-CSF treatment, gene expression analysis, and statistical methods, are comprehensively described in *SI Appendix*, Materials and Methods.

Data, Materials, and Software Availability. RNAseq data in raw format, prior to postprocessing and analysis, generated in this study are deposited in the Gene Expression Omnibus (accession number GSE277716) (48). All study data are included in the article and/or *SI Appendix*.

ACKNOWLEDGMENTS. We would like to thank the Flow Cytometry & Fluorescence Activated Cell Sorting Core, the Digestive Diseases Research Core Center (DDRCC), the Alafi Neuroimaging Laboratory (supported by an NIH Shared Instrumentation Grant S10 OD032131), the Molecular Microbiology Imaging Facility, and the Immunomonitoring Laboratory at the Bursky Center for Human Immunology and Immunotherapy Programs (supported by the Rheumatic Diseases Core Center, NIH WLC6313040077) at Washington University School of Medicine. This study was supported by the NIH (R01DK126969, R01DK132327, R01DK30292), the Pew Charitable Trusts (00035299), and the São Paulo Research Foundation, Brazil (FAPESP 2017/06577-9, 2018/15313-8, 2021/09155-3, and 2023/00393-4).

Author affiliations: [a]Department of Pathology and Immunology, Washington University School of Medicine, St Louis, MO 63110; [b]Department of Genetics, Evolution, Microbiology, and Immunology, Institute of Biology, University of Campinas, Campinas, SP 13083-862, Brazil; and [c]Department of Anesthesiology, Children's Hospital, Zhejiang University School of Medicine, National Clinical Research Center for Child Health, Hangzhou 310052, China

1. M. C. Abt, P. T. McKenney, E. G. Pamer, Clostridium difficile colitis: Pathogenesis and host defence. *Nat. Rev. Microbiol.* **14**, 609–620 (2016).
2. W. K. Smits, D. Lyras, D. B. Lacy, M. H. Wilcox, E. J. Kuijper, Clostridium difficile infection. *Nat. Rev. Dis. Primers* **2**, 16020 (2016).
3. C. Normington, C. H. Chilton, A. M. Buckley, Clostridioides difficile infections; new treatments and future perspectives. *Curr. Opin. Gastroenterol.* **40**, 7–13 (2024).
4. B. Vakili, A. Fateh, H. Asadzadeh Aghdaei, F. Sotoodehnejadnematalahi, S. D. Siadat, Characterization of Gut Microbiota in Hospitalized Patients with Clostridioides difficile Infection. *Curr. Microbiol.* **77**, 1673–1680 (2020).
5. C. M. Theriot *et al.*, Antibiotic-induced shifts in the mouse gut microbiome and metabolome increase susceptibility to Clostridium difficile infection. *Nat. Commun.* **5**, 3114 (2014).
6. R. Chandrasekaran, D. B. Lacy, The role of toxins in Clostridium difficile infection. *FEMS Microbiol. Rev.* **41**, 723–750 (2017).
7. S. L. Kordus, A. K. Thomas, D. B. Lacy, Clostridioides difficile toxins: Mechanisms of action and antitoxin therapeutics. *Nat. Rev. Microbiol.* **20**, 285–298 (2022).
8. J. Czepiel *et al.*, Clostridium difficile infection: Review. *Eur. J. Clin. Microbiol. Infect. Dis.* **38**, 1211–1221 (2019).
9. M. Hasegawa *et al.*, Nucleotide-binding oligomerization domain 1 mediates recognition of Clostridium difficile and induces neutrophil recruitment and protection against the pathogen. *J. Immunol.* **186**, 4872–4880 (2011).
10. M. Hasegawa *et al.*, Protective role of commensals against Clostridium difficile infection via an IL-1β-mediated positive-feedback loop. *J. Immunol.* **189**, 3085–3091 (2012).
11. T. Griseri, B. S. McKenzie, C. Schiering, F. Powrie, Dysregulated hematopoietic stem and progenitor cell activity promotes interleukin-23-driven chronic intestinal inflammation. *Immunity* **37**, 1116–1129 (2012).
12. T. Griseri *et al.*, Granulocyte macrophage colony-stimulating factor-activated eosinophils promote interleukin-23 driven chronic colitis. *Immunity* **43**, 187–199 (2015).
13. C. Pearson *et al.*, ILC3 GM-CSF production and mobilisation orchestrate acute intestinal inflammation. *Elife* **5**, e10066 (2016).
14. J. A. Hamilton, Colony-stimulating factors in inflammation and autoimmunity. *Nat. Rev. Immunol.* **8**, 533–544 (2008).
15. K. Uchida *et al.*, GM-CSF autoantibodies and neutrophil dysfunction in pulmonary alveolar proteinosis. *N Engl. J. Med.* **356**, 567–579 (2007).
16. J. L. Fachi, M. A. R. Vinolo, M. Colonna, Reviewing the clostridioides difficile mouse model: Insights into infection mechanisms. *Microorganisms* **12**, 273 (2024).
17. J. L. Fachi *et al.*, Acetate coordinates neutrophil and ILC3 responses against C. difficile through FFAR2. *J. Exp. Med.* **217**, jem.20190489 (2020).
18. M. C. Abt *et al.*, Innate immune defenses mediated by two ILC subsets are critical for protection against acute clostridium difficile infection. *Cell Host Microbe* **18**, 27–37 (2015).
19. E. Vivier *et al.*, Innate lymphoid cells: 10 years on. *Cell* **174**, 1054–1066 (2018).
20. M. Colonna, Innate lymphoid cells: diversity, plasticity, and unique functions in immunity. *Immunity* **48**, 1104–1117 (2018).
21. M. Cella *et al.*, A human natural killer cell subset provides an innate source of IL-22 for mucosal immunity. *Nature* **457**, 722–725 (2009).
22. G. Eberl, M. Colonna, J. P. Di Santo, A. N. J. McKenzie, Innate lymphoid cells. Innate lymphoid cells: A new paradigm in immunology. *Science* **348**, aaa6566 (2015).
23. A. Diefenbach, M. Colonna, S. Koyasu, Development, differentiation, and diversity of innate lymphoid cells. *Immunity* **41**, 354–365 (2014).
24. C. Vonarbourg *et al.*, Regulated expression of nuclear receptor RORγt confers distinct functional fates to NK cell receptor-expressing RORγt(+) innate lymphocytes. *Immunity* **33**, 736–751 (2010).
25. G. Sciumé *et al.*, Distinct requirements for T-bet in gut innate lymphoid cells. *J. Exp. Med.* **209**, 2331–2338 (2012).
26. C. S. N. Klose *et al.*, A T-bet gradient controls the fate and function of CCR6-RORγt+ innate lymphoid cells. *Nature* **494**, 261–265 (2013).
27. A. Mortha *et al.*, Microbiota-dependent crosstalk between macrophages and ILC3 promotes intestinal homeostasis. *Science* **343**, 1249288 (2014).
28. J. Qiu *et al.*, The aryl hydrocarbon receptor regulates gut immunity through modulation of innate lymphoid cells. *Immunity* **36**, 92–104 (2012).
29. J. S. Lee *et al.*, AHR drives the development of gut ILC22 cells and postnatal lymphoid tissues via pathways dependent on and independent of Notch. *Nat. Immunol.* **13**, 144–151 (2011).
30. L. E. Collins *et al.*, Surface layer proteins isolated from Clostridium difficile induce clearance responses in macrophages. *Microbes Infect.* **16**, 391–400 (2014).
31. H. Chan *et al.*, Vitamin D3 and carbamazepine protect against Clostridioides difficile infection in mice by restoring macrophage lysosome acidification. *Autophagy* **18**, 2050–2067 (2022).
32. S. J. Aujla *et al.*, IL-22 mediates mucosal host defense against Gram–negative bacterial pneumonia. *Nat. Med.* **14**, 275–281 (2008).
33. P. J. Dubin, J. K. Kolls, Th17 cytokines and mucosal immunity. *Immunol. Rev.* **226**, 160–171 (2008).
34. M. Metzemaekers, M. Gouwy, P. Proost, Neutrophil chemoattractant receptors in health and disease: Double-edged swords. *Cell Mol. Immunol.* **17**, 433–450 (2020).
35. K. M. C. Lee, A. A. Achuthan, J. A. Hamilton, GM-CSF: A promising target in inflammation and autoimmunity. *Immunotargets Ther.* **9**, 225–240 (2020).
36. J. Fleischmann, D. W. Golde, R. H. Weisbart, J. C. Gasson, Granulocyte-macrophage colony-stimulating factor enhances phagocytosis of bacteria by human neutrophils. *Blood* **68**, 708–11 (1986).
37. C. Costantini *et al.*, Neutrophil activation and survival are modulated by interaction with NK cells. *Int. Immunol.* **22**, 827–838 (2010).
38. T. Castro-Dopico *et al.*, GM-CSF Calibrates Macrophage Defense and Wound Healing Programs during Intestinal Infection and Inflammation. *Cell Rep.* **32**, 107857 (2020).
39. W. Elsegeiny *et al.*, Murine models of Pneumocystis infection recapitulate human primary immune disorders. *JCI Insight* **3**, e91894 (2018).
40. W. Sheng *et al.*, STAT5 programs a distinct subset of GM-CSF-producing T helper cells that is essential for autoimmune neuroinflammation. *Cell Res.* **24**, 1387–1402 (2014).
41. C. Song *et al.*, Unique and redundant functions of NKp46+ ILC3s in models of intestinal inflammation. *J. Exp. Med.* **212**, 1869–1882 (2015).
42. P. Sah, B. A. Knighten, M. A. Reidy, L. A. Zenewicz, Polyamines and hypusination are important for Clostridioides difficile toxin B (TcdB)-mediated activation of group 3 innate lymphocytes (ILC3s). *Infect. Immun.* **91**, e0023623 (2023).
43. S. Jose, R. Madan, Neutrophil-mediated inflammation in the pathogenesis of Clostridium difficile infections. *Anaerobe* **41**, 85–90 (2016).
44. J. Li *et al.*, Activation of DR3 signaling causes loss of ILC3s and exacerbates intestinal inflammation. *Nat. Commun.* **10**, 3371 (2019).
45. D. Croxatto *et al.*, Group 3 innate lymphoid cells regulate neutrophil migration and function in human decidua. *Mucosal. Immunol.* **9**, 1372–1383 (2016).
46. S. M. Bal, K. Golebski, H. Spits, Plasticity of innate lymphoid cell subsets. *Nat. Rev. Immunol.* **20**, 552–565 (2020).
47. M. Cella *et al.*, Subsets of ILC3–ILC1-like cells generate a diversity spectrum of innate lymphoid cells in human mucosal tissues. *Nat. Immunol.* **20**, 980–991 (2019).
48. J. L. Fachi *et al.*, NKp46+ ILC3s promote early neutrophil defense against *Clostridioides difficile* infection through GM-CSF secretion. *Proc. Natl. Acad. Sci. U.S.A.* **121**, e2416182121 (2024).